The Journal of Chemical Physics ARTICLE scitation.org/journal/jcp

SparseMaps—A systematic infrastructure for reduced-scaling electronic structure methods. VI. Linear-scaling explicitly correlated N-electron valence state perturbation theory with pair natural orbital

Cite as: J. Chem. Phys. 158, 124120 (2023); doi: 10.1063/5.0144260
Submitted: 28 January 2023 • Accepted: 13 March 2023 •
Published Online: 30 March 2023

Yang Guo,[1] Fabijan Pavošević,[2] Kantharuban Sivalingam,[3] Ute Becker,[3] Edward F. Valeev,[4] and Frank Neese[3,a)]

AFFILIATIONS

[1] Qingdao Institute for Theoretical and Computational Sciences, Institute of Frontier and Interdisciplinary Science, Shandong University, Qingdao, Shandong 266237, China
[2] Center for Computational Quantum Physics, Flatiron Institute, 162, 5th Ave., New York, New York 10010, USA
[3] Max Planck Institut für Kohlenforschung, Kaiser-Wilhelm-Platz 1, D-45470 Mülheim an der Ruhr, Germany
[4] Department of Chemistry, Virginia Tech, Blacksburg, Virginia 24061, USA

[a)] **Author to whom correspondence should be addressed:** Frank.Neese@kofo.mpg.de

ABSTRACT

In this work, a linear scaling explicitly correlated N-electron valence state perturbation theory (NEVPT2-F12) is presented. By using the idea of a domain-based local pair natural orbital (DLPNO), computational scaling of the conventional NEVPT2-F12 is reduced to near-linear scaling. For low-lying excited states of organic molecules, the excitation energies predicted by DLPNO-NEVPT2-F12 are as accurate as the exact NEVPT2-F12 results. Some cluster models of rhodopsin are studied using the new algorithm. Our new method is able to study systems with more than 3300 basis functions and an active space containing 12 π-electrons and 12 π-orbitals. However, even larger calculations or active spaces would still be feasible.

I. INTRODUCTION

The accuracy of quantum chemical calculations relies first and foremost on the quality of the underlying theoretical approach. However, in practice, it has proven to be unavoidable to construct many particle wave functions with the help of one-particle wave functions (orbitals) and, moreover, to expand the orbitals in terms of one-particle basis sets. The latter would need to be mathematically complete for the chosen theoretical method to deliver its "intended" result. However, in practice, one can only handle incomplete basis sets and, hence, the error associated with a given calculation contains an error from the method itself and an error due to the basis set incompleteness; these errors are not necessarily additive. While a great deal has been learned about the behavior of basis set incompleteness errors in practical applications, it would still be desirable to eliminate this error source to the largest possible extent.

Unfortunately, it is well known that the correlation energies of single-reference (SR) and multireference (MR) methods converge slowly with the size of the basis sets. In 1986, Davidson and Feller observed that in order to obtain even qualitatively correct relative energies, double-ξ basis sets are not sufficient.[1] Moreover, to attain chemical accuracy, the basis set error must be nearly completely suppressed by reaching the complete basis set (CBS) limit.[2]

There are two principal approaches to estimate the CBS limit: (a) basis set extrapolation[2–4] and (b) the explicitly correlated

methods.[5] In the extrapolation methods, one empirically estimates the CBS limit from the energies obtained from a systematically designed series of basis sets. The most common extrapolation scheme is due to Helgaker and involves a two-point extrapolation with a cubic dependence on the cardinal number.[2] The extrapolation formula also makes it easy to extrapolate any property to the basis set limit that can be written as an energy derivative, for example, dipole moments[6] or nuclear gradients.[7]

The second way to overcome the incomplete basis set problem is through the explicitly correlated theory, known as R12 or, more generally, the F12 theory.[8] In the F12 theory, the conventional orbital-based correlated wave functions are supplemented by terms explicitly containing the inter-electronic distances. These methods were introduced by Kutzelnigg *et al.* on the basis of the partial wave expansion of atomic correlation energies[5] and were originally referred to as linear R12 methods (due to the use of linear dependence on the inter-electronic distances).[9–11] A difficult problem in these theories is the occurrence of three- and four-electron integrals that are difficult to compute and exceedingly numerous, thus preventing the methods from being applicable to mainstream computational chemistry.[10] Although the resolution of identity (RI) approximation was introduced by Kutzelnigg and Klopper to avoid the evaluation of electronic coordinate-coupled integrals, very large orbital basis sets (OBS) must be used to achieve accurate CBS limit results.[12] Thus, Klopper and Samson introduced the "auxiliary basis set" (ABS) for the RI to reduce the errors arising from a standard OBS in R12 calculations.[13] Later, one of us (EV) introduced the so-called "complementary auxiliary basis set" (CABS) basis set to further reduce the errors due to the RI.[14] In the original R12 method, the linear r_{12} operator is used. In 2004, Ten-no introduced the Slater-type geminal to replace the linear r_{12} operator, which greatly improves the accuracy of R12.[15,16] These, together with the introduction of a rational generator ansatz,[17] resulted in modern F12 methods that are efficient and robustly applicable.[18–21]

In previous work, some of us performed a systematic comparison between the two methods, F12 and extrapolation methods, at the MP2 level.[22] Both the F12 and extrapolation methods were found to be able to predict accurate absolute and relative energies. In this comparison, the extrapolation method was found to be computationally slightly more efficient than the MP2-F12 method, whereas the F12 method produces slightly better reaction energies. This, of course, is specific to MP2. At any higher level of wave function theory, the F12 method is far more efficient than extrapolation. However, there is another advantage of the F12 method. In the F12 theory, not only the CBS limit properties can be computed but also the CBS limit many-particle wave functions are obtained. Thus, various properties based on the F12 wave functions can be conveniently evaluated. Recently, Werner *et al.* implemented the analytical gradients of F12 theories for geometry optimization calculations.[23,24]

In the last decades, the F12 theory has turned into a mature theory that is widely used in actual computational chemistry studies. Various explicitly correlated MR methods have been developed as well.[25–37] Although the computational cost of state-of-the-art F12 methods has been significantly reduced by avoiding the evaluation of three- and four-electron integrals, these methods are still computationally expensive. The CABS basis set, also known as the "OptRI" basis set,[51] is considered to be a near-complete auxiliary basis set for essentially any underlying OBS. Different kinds of integrals involving the OBS and CABS basis functions have to be evaluated in the F12 calculations, which introduces an additional computational overhead compared to the parent correlation calculations. To overcome this difficulty, explicitly correlated "direct" local MP2 methods were developed by Werner and Manby.[38,39] Subsequently, Adler and Werner extended the idea to the explicitly correlated coupled cluster theory as well.[40,41] In these works, the projected atomic orbitals (PAOs) and the corresponding truncated CABS are used to reduce the size of virtual space and CABS space, respectively.[39] However, the pre-factors of these algorithms are still large, which is due to the size of the PAO domains.

Pair natural orbitals (PNOs) were introduced into quantum chemistry early on, as a concise way to represent the many-particle wave function in the most compact way.[42] Realizing PNOs are more compact than PAOs, some of us started to utilize PNOs in various local correlation methods since 2009.[43–46] Today, PNOs are widely used in linear or low-scaling correlation methods by our group,[47–50] our collaborators,[51,52] and many[53] other groups.[54–56] In addition, various PNO-based explicitly correlated local perturbation theories (MP2-F12) and coupled cluster algorithms (CCSD-F12) are reported.[55–61] These methods are now widely used by computational chemists with hundreds, if not thousands, of reported studies in existence.

In 2015, we introduced the "SparseMaps" infrastructure, to simplify and formalize the use of sparsity in local methods of any kind. These SparseMaps were the cornerstone that allowed the development of linear scaling domain-based local PNO (DLPNO) methods.[47] Employing SparseMaps, both the construction and storage of the RI integral are reduced, which increases linearly with the size of systems.[47] Various SR and MR DLPNO algorithms have been developed based on SparseMaps.[47–50,62–65] Among them, two linear scaling explicitly correlated SR methods, DLPNO-MP2-F12 and DLPNO-CCSD-F12, are available.[50,62]

Although a number of explicitly correlated MR methods, including CASPT2-F12,[33] N-electron valence state perturbation theory (NEVPT2)-F12,[37] and MRCI-F12,[34] have been implemented, a linear scaling MR-F12 method has not been reported in the literature. In the present work, based on the idea of DLPNO, a linear scaling explicitly correlated N-electron valence state perturbation theory (NEVPT2-F12) is developed. Compared to the strongly contracted NEVPT2 variant,[66] the fully internally contracted (FIC-) NEVPT2 (also known as partially contracted NEVPT2) method is unitarily invariant with respect to the rotations within doubly occupied and virtual spaces.[67–69] We found that, by using local inactive MOs, the errors due to the non-invariance of SC-NEVPT2 may be problematic.[49] Thus, only local FIC-NEVPT2-F12 (DLPNO-NEVPT2-F12) will be discussed in the present work. After an introduction to the DLPNO-NEVPT2-F12 theory, the three key truncation parameters are carefully redesigned. Subsequently, vertical excitation energies of a few organic molecules are studied using the DLPNO-NEVPT-F12 algorithm. Finally, cluster models containing the 11-cis retinal chromophore are studied.

II. THEORY AND IMPLEMENTATION

In the present work, i, j, k, l and t, u, v, w denote the doubly occupied and active MOs, respectively. Indices a, b, c, d denote conventional virtual orbitals (or semi-canonical PNOs), whereas

$\alpha, \beta, \gamma, \delta$ are CABS indices orthonormal to the OBS (or pair-specific ones). The indices p, q, r, s label arbitrary MOs. The formalism of NEVPT2-F12 was presented in our previous work.[37] Here, only the basic framework of NEVPT2-F12 is recapped. The 0-order NEVPT wave function is defined as a superposition of configuration state functions (CSF) or Slater determinants,

$$|0\rangle = \sum_I C_I |\Phi_I\rangle, \tag{1}$$

which is usually generated by a complete active space configuration interaction (CASCI) or a complete active space self-consistent field (CASSCF) calculation. The 0-order Hamiltonian used in NEVPT is the Dyall Hamiltonian,[67]

$$H^{Dyall} = \sum_{ij} F_{ij} E_i^j + \sum_{ab} F_{ab} E_a^b + \sum_{tu} F_{tu} E_u^t + \frac{1}{2} \sum_{tuvw} (tv|uw)(E_v^t E_w^u - \delta_v^u E_w^t) + C, \tag{2}$$

where the spin-free second quantized replacement operator is defined as $E_q^p = a_{p_\alpha}^+ a_{q_\alpha} + a_{p_\beta}^+ a_{q_\beta}$, and C in Eq. (2) is the constant defined elsewhere.[66] In the doubly occupied and virtual space, the Hamiltonian reduces to the one-body Fock operator. The 1-order NEVPT wave function has contributions from eight distinct subspaces. The definition of internally contracted 1-order wave functions of both NEVPT and NEVPT-F12 are shown in Fig. 1. Since the basis set error due to the two internal subspaces is small and rapidly convergent, only the remaining six subspaces need to include F12 corrections. Note that the single excitation components of semi-external subspaces have to be projected out of the F12 wave functions. The $W_{pq}^{\alpha\beta}$ in the F12 wave functions are correlation operators defined in the previous work.[37]

With the FIC wave functions shown in Fig. 1, the working equations of NEVPT2-F12 are derived following the same steps as in the parent NEVPT2. The simplified residual equations and energy expressions of the NEVPT2-F12 ansatz are given in the supplementary material. The amplitudes T_{pq}^{rs} of the first-order wave function are obtained by solving the NEVPT2-F12 residual equations. As in MP2-F12, the NEVPT2 and F12 residual equations within a subspace are coupled and, thus, in principle, have to be solved iteratively. The two residual equations decouple with the fixed amplitude approximation[17] that is used in this work to determine the F12 amplitudes. Provided that canonical MOs are used to represent inactive spaces, the NEVPT2 amplitudes can be computed directly without any iteration as well.

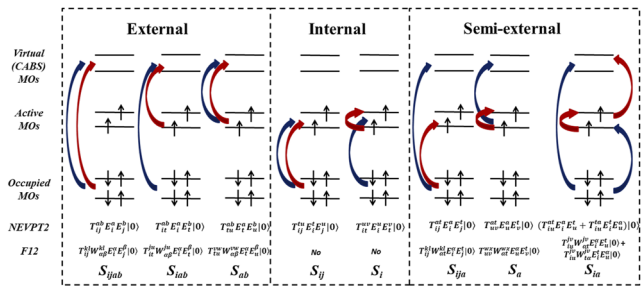

FIG. 1. The eight first-order interaction subspaces and the corresponding first-order wave functions of NEVPT2 and F12.

However, DLPNO methods use semi-canonical PNOs for the pair-specific virtual space and localized MOs (LMOs) for the doubly occupied space.[45,47] Thus, the equations shown in the supplementary material, S1, refer to doubly occupied LMOs and canonical virtual MOs. The NEVPT2-F12 energies computed using these equations are unitarily invariant with respect to rotations of doubly occupied MOs and rotations of active MOs. As shown in the previous work,[49] such a formulation can be used in the DLPNO-NEVPT2 algorithm with minor modifications. Following the same strategy, it is straightforward to translate these NEVPT2-F12 equations into the DLPNO version. The explicit expressions of the S_{iab} subspace of DLPNO-NEVPT2-F12 are given in the supplementary material, S2, as well.

III. RESULTS

The aforementioned DLPNO-NEVPT2-F12 algorithm is implemented in a parallelized fashion in a development version of the ORCA program suite based on ORCA 5.0.[70,71] All correlation calculations are carried out with the frozen core approximation. In all F12 calculations, the cc-pVXZ-F12 (X = D, T, and Q) basis sets with the matching CABS basis sets cc-pVXZ-F12/OptRI are employed and abbreviated as "XZ."[72,73] The aug-cc-pVXZ basis sets are used to compute various two-electron integrals in NEVPT2-F12 under the RI approximation. In all F12 calculations, including DLPNO-NEVPT2-F12, the canonical CABS single correction ($[2]_s$)[74] to the basis set errors of CASSCF is considered. All calculations are performed on clusters with a single core of Intel i7-6700HQ central processing unit (CPU) (2.60 GHz).

A. Selection of thresholds

Like DLPNO-NEVPT2,[49] there are three major parameters in the DLPNO-NEVPT2-F12 algorithm, a threshold to truncate PNOs (***TCutPNO***), and two thresholds, ***TCutMKN*** and ***TCutDO***, for the construction of sparse maps. The parameter ***TCutMKN*** is used to truncate the density fitting domains, and ***TCutDO*** controls the size of the virtual space for each occupied or active MO. To determine the recommended values of the three parameters, the lowest singlet and triplet states of two diradical molecules, $[(C_4SH_3)\text{-}(C_4SH_3)]^{2+}$ (referred to as Thio_00) and $[(C_4SH_3)\text{-}C_{10}H_{20}\text{-}(C_4SH_3)]^{2+}$ (referred to as Thio_10), are used.[49] State-averaged (SA) CASSCF wave functions over the lowest singlet and triplet states are used as references. The active spaces involving the two molecules contain the valence 10 π-electrons and 10 π-orbitals. In the present subsection, the CASSCF and $[2]_s$ energies are not considered.

The total DLPNO-NEVPT2-F12 correlation energy can be divided into the NEVPT2 and F12 parts. The convergence trends of NEVPT2, F12, and whole NEVPT2-F12 correlation energy using different ***TCutPNO*** parameters are given in Fig. 2. One can see that the results of the singlet and triplet states overlap for both systems. Thus, the DLPNO-NEVPT2-F12 method is able to capture the same ratio of correlation energies for different states and deliver accurate excitation energies. The F12 correction energies converge slower than NEVPT2 energies with ***TCutPNO***. By setting ***TCutPNO*** as 10^{-8}, around 99.6% of F12 correction energies are recovered by DLPNO-F12, whereas more than 99.95% of NEVPT2 correlation energies are reproduced. Since the total NEVPT2-F12 correlation

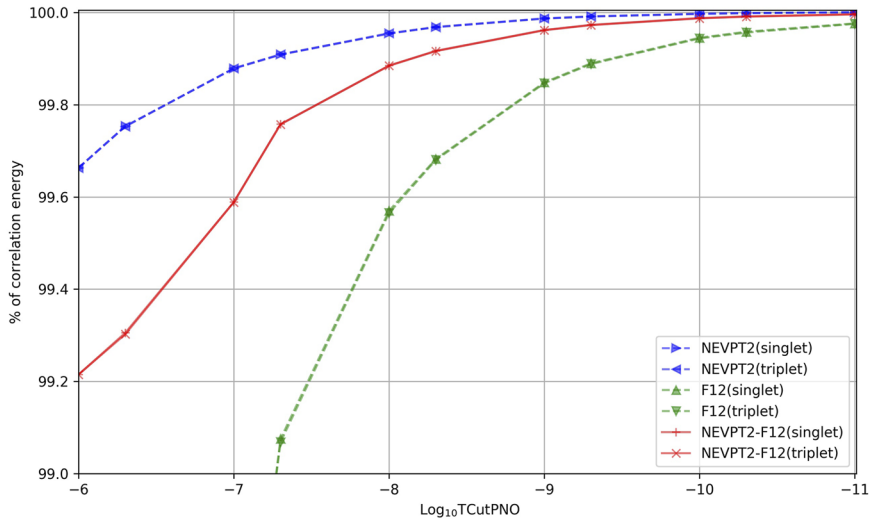

(a)

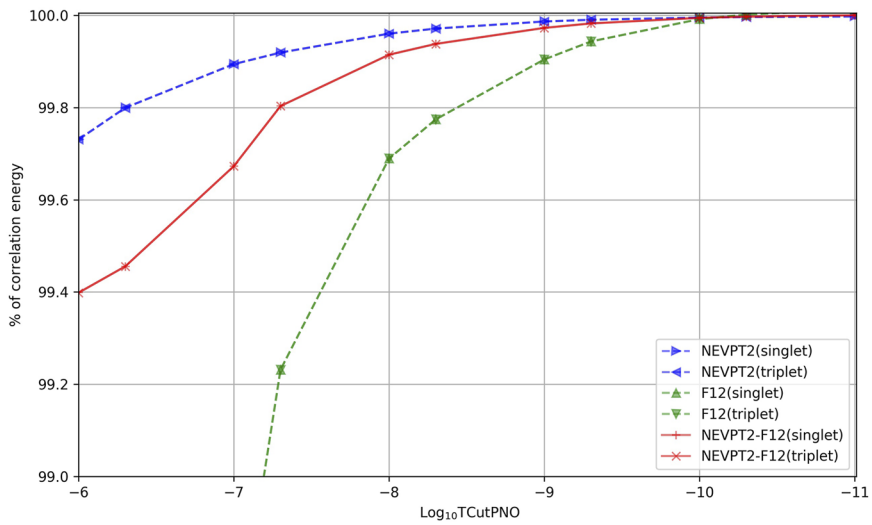

(b)

FIG. 2. The DLPNO-NEVPT2-F12 correlation energy ratio of (a) Thio_00 and (b) Thio_10 recovered by different ***TCutPNO*** thresholds. The NEVPT2 and F12 parts are given separately.

energies are dominated by the NEVPT2 parts, about 99.9% of overall NEVPT2-F12 energies are recovered using the DLPNO algorithm. Thus, 10^{-8} is chosen as the default setting of ***TCutPNO***. Interestingly, the DLPNO-NEVPT2-F12 results of Thio_10 are slightly more accurate than those of Thio_00. This might be due to the valence electrons in Thio_00 being relatively more delocalized than in Thio_10.

By setting ***TCutPNO*** as 10^{-8}, the percentage of DLPNO-NEVPT-F12 results utilizing different ***TCutMKN*** and ***TCutDO*** thresholds are given in Figs. 3 and 4, respectively. Again, the algorithm always describes singlet and triplet states with the same accuracy. It is evident that using the settings ***TCutMKN*** = 10^{-3} and ***TCutDO*** = 10^{-2}, the accuracy of the DLPNO-NEVPT2-F12 algorithm is not influenced by the truncations. Thus, the default setting of parameters ***TCutMKN*** and ***TCutDO*** is 10^{-3} and 10^{-2}, respectively. Using these default thresholds, about 99.9% of the total NEVPT2-F12 energies can be recovered.

B. Benchmark calculations

To validate the new algorithm, several organic molecules (including furan, pyrrole, imidazole, benzene, and octatetraene) from Thiel's test set are studied,[75] whose basis set errors are somewhat larger than the other molecules in the test set.[76] The active space and the protocol to compute excitation energies are identical to the original work.[75] Thus, SA and state-specific (SS) energies of the ground states are computed. The NEVPT2 results using cc-pVXZ (X = D, T, and Q) are computed for comparison. The

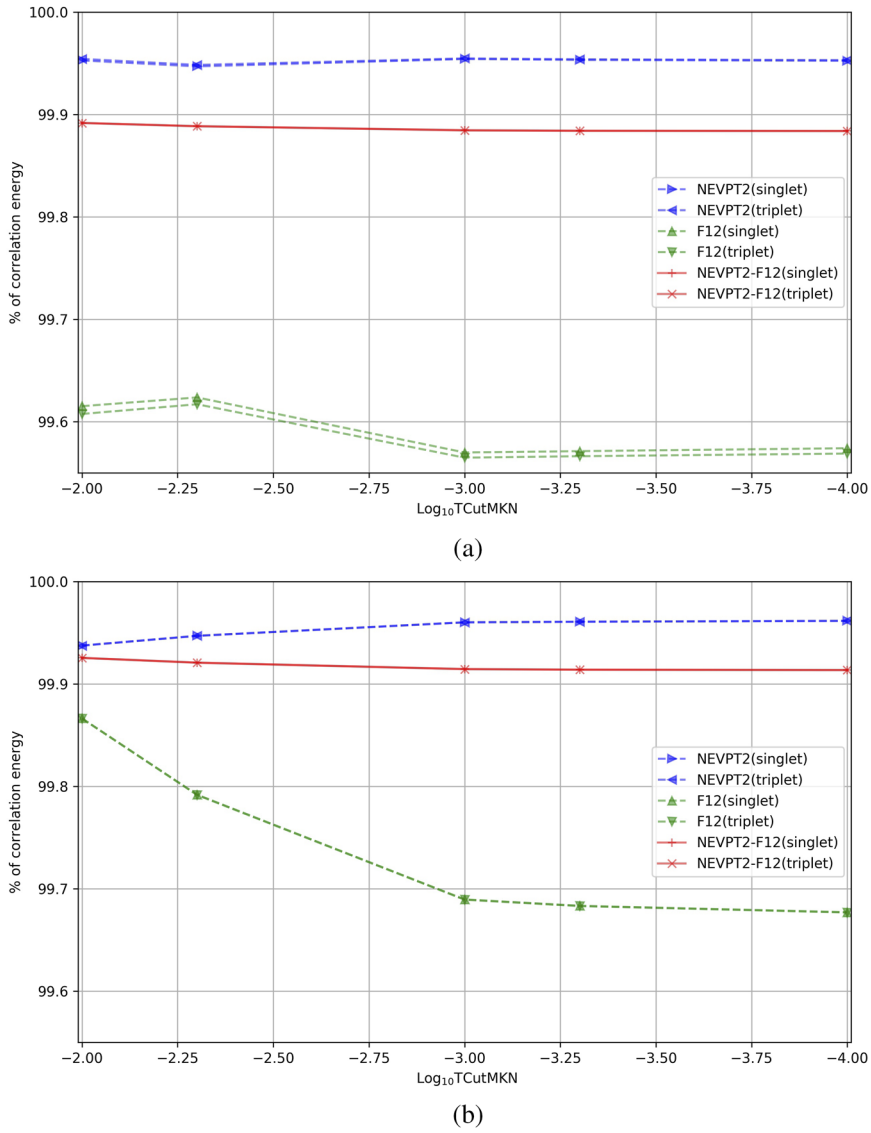

FIG. 3. The DLPNO-NEVPT2-F12 correlation energy ratio of (a) Thio_00 and (b) Thio_10 recovered by different ***TCutMKN*** thresholds. The ***TCutPNO*** is fixed at 10^{-8}.

CBS limit results of CASSCF and NEVPT2 are computed based on the 4–5 extrapolation methods reported by Varandas[77] and Helgaker,[2] respectively. The deviations of absolute energies from various NEVPT2 and NEVPT2-F12 calculations with respect to the CBS limit are given in Table I. The results depict that both NEVPT2-F12 and DLPNO-NEVPT2-F12 methods produce much more accurate absolute results than NEVPT2 does. The DLPNO-NEVPT2-F12 and canonical NEVPT2-F12 numbers are almost indistinguishable. The mean absolute deviations (MADs) and standard deviations (SDs) of DLPNO-NEVPT2-F12 relative to the CBS limit are less than 0.6 eV with a DZ basis set, which are more accurate than the NEVPT2 results with cc-pVQZ basis sets. As expected, both NEVPT2-F12 and DLPNO-NEVPT2-F12 calculations with a QZ basis set predict the most satisfactory results. Both statistical measures are less than 0.04 eV.

We also computed the CBS limit NEVPT2 results employing 3–4 extrapolations. The statistical results can be found in S3 of the supplementary material. NEVPT2-F12 with the QZ basis set produces lower absolute energies than those obtained by 3–4 extrapolations. This leads to apparently larger deviations. The CBS limit results computed using an alternative extrapolation method proposed by Valeev *et al.* can be found in S3 as well.[78] In these extrapolation methods, the parameters are optimized for SR dynamic correlation methods[2] and might not be suitable for the extrapolation of MR dynamic correlation energies. To address this question, we studied the correlation energy convergence trends of NEVPT2. The decay of the NEVPT2 correlation energies of the benzene molecule is given in Fig. S4 of the supplementary material. The correlation energy of the S_{ijab} subspace should decay cubically with the cardinal number as SR MP2 and this is what is observed. However, the

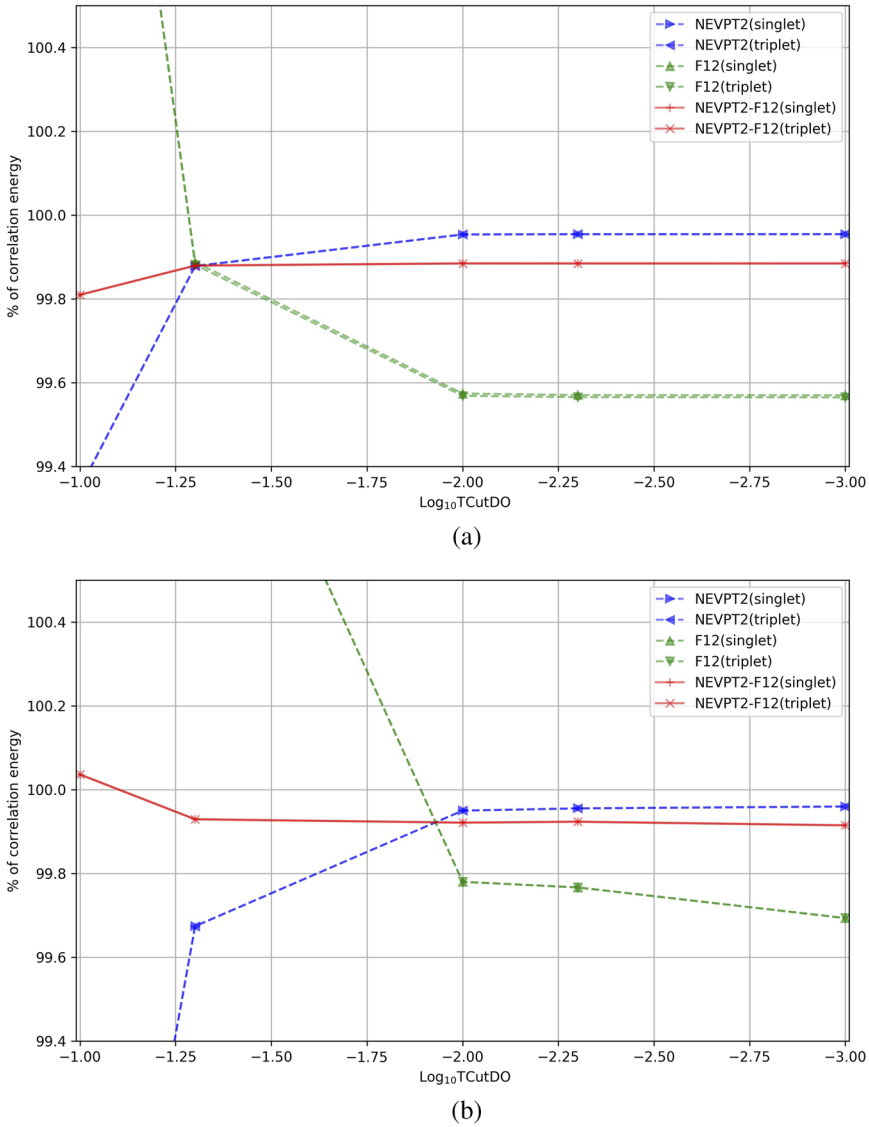

FIG. 4. The DLPNO-NEVPT2-F12 correlation energy ratio of (a) Thio_00 and (b) Thio_10 recovered by different ***TCutDO*** thresholds. The ***TCutPNO*** is fixed at 10^{-8}.

correlation energy convergence behaviors of the other subspaces are slightly different from that of the S_{ijab} subspace. Since the convergence rates are different, we conclude that the extrapolation of the NEVPT2 correlation energies should be performed for each subspace separately. We will come back to this subject in future work. Nevertheless, the extrapolation errors due to the other seven subspaces should be small, as long as the 4–5 extrapolation method is used.

The excitation energies of these molecules are given in Table II. The MADs of all F12 algorithms are close, from 0.02 to 0.03 eV, whereas the MAD of NEVPT2 results with QZ basis set regarding the CBS limit results is 0.06 eV. Both NEVPT2-F12 and DLPNO-NEVPT2-F12 deliver more accurate excitation energies than NEVPT2 with a QZ basis set. The newly developed DLPNO-NEVPT2-F12 produces the same absolute and relative energies as the conventional NEVPT2-F12 for these molecules. The DLPNO-NEVPT2-F12 results with a DZ basis set can already deliver absolute and relative energies that are more accurate than the NEVPT2 calculations with the QZ basis set.

C. Scaling behavior

The scaling behavior of the present DLPNO-NEVPT2-F12 algorithm is studied by using a series of $[(C_4SH_3)\text{-}C_nH_{2n}\text{-}(C_4SH_3)]^{2+}$ molecules with CASSCF(10, 10) references and a DZ basis set. The wall time comparison between canonical NEVPT2-F12 (NEVPT2) and DLPNO-NEVPT2-F12 (DLPNO-NEVPT2) is shown in Fig. 5. It is encouraging that the crossover point between DLPNO-NEVPT-F12 and DLPNO-NEVPT2 already occurs at a very small system size of about 10 atoms. By contrast, we found that

TABLE I. The absolute energies of low-lying excited states of the chosen organic molecules. The NEVPT2, NEVPT2-F12, and DLPNO-NEVPT2-12 results are deviations (in eV) with respect to that of the CBS limit.

		NEVPT2			NEVPT2-F12			DLPNO-NEVPT2-F12			
Molecule	States	DZ	TZ	QZ	DZ	TZ	QZ	DZ	TZ	QZ	CBS limit (Hartree)
Furan	SS 1^1A_1	9.38	3.34	1.37	0.59	0.10	−0.02	0.60	0.11	0.00	−229.700 41
	SA 1^1A_1	9.48	3.41	1.42	0.62	0.12	0.01	0.64	0.14	0.02	−229.706 50
	2^1A_1	9.64	3.44	1.43	0.61	0.12	0.00	0.63	0.13	0.01	−229.460 15
	3^1A_1	10.03	3.66	1.56	0.58	0.07	−0.06	0.61	0.09	−0.04	−229.411 00
	1^1B_2	10.13	3.76	1.64	0.55	0.01	−0.16	0.57	0.03	−0.14	−229.482 30
	1^3A_1	9.51	3.38	1.39	0.60	0.11	−0.01	0.62	0.12	0.01	−229.494 73
	1^3B_2	9.52	3.39	1.39	0.60	0.10	−0.01	0.62	0.12	0.00	−229.542 43
Pyrrole	SS 1^1A_1	8.65	3.09	1.26	0.49	0.08	−0.01	0.51	0.10	0.00	−209.848 18
	SA 1^1A_1	8.71	3.13	1.29	0.51	0.09	0.00	0.53	0.11	0.01	−209.850 88
	2^1A_1	8.91	3.20	1.32	0.51	0.09	−0.01	0.53	0.11	0.01	−209.611 80
	3^1A_1	9.28	3.40	1.44	0.48	0.05	−0.06	0.50	0.07	−0.05	−209.560 90
	1^1B_2	9.30	3.44	1.48	0.43	−0.01	−0.11	0.45	0.01	−0.10	−209.613 50
	1^3A_1	8.82	3.15	1.29	0.51	0.09	−0.01	0.53	0.11	0.01	−209.641 68
	1^3B_2	8.80	3.14	1.29	0.50	0.08	−0.01	0.52	0.10	0.00	−209.675 39
Imidazole	SS $1^1A'$	9.19	3.30	1.35	0.53	0.09	−0.02	0.55	0.10	−0.01	−225.893 36
	SA $1^1A'$	9.34	3.41	1.42	0.57	0.11	0.01	0.58	0.12	0.02	−225.899 84
	$2^1A'$	9.58	3.50	1.47	0.56	0.10	−0.01	0.58	0.11	0.00	−225.651 97
	$3^1A'$	9.68	3.52	1.46	0.51	0.04	−0.06	0.53	0.06	−0.05	−225.653 92
	$4^1A'$	9.73	3.56	1.49	0.49	0.01	−0.11	0.51	0.03	−0.09	−225.590 93
	$1^1A''$	9.47	3.41	1.41	0.58	0.10	−0.01	0.60	0.12	0.01	−225.644 35
	$2^1A''$	9.54	3.45	1.43	0.58	0.10	−0.02	0.60	0.12	0.00	−225.607 91
	$1^3A'$	9.39	3.38	1.39	0.56	0.10	0.00	0.58	0.12	0.01	−225.719 84
	$2^3A'$	9.45	3.40	1.40	0.57	0.11	0.00	0.59	0.13	0.01	−225.680 33
	$3^3A'$	9.55	3.44	1.42	0.58	0.11	0.00	0.60	0.13	0.01	−225.658 33
	$4^3A'$	9.45	3.40	1.40	0.57	0.11	0.00	0.58	0.12	0.01	−225.637 30
	$1^3A''$	9.41	3.38	1.39	0.58	0.10	−0.01	0.59	0.12	0.01	−225.661 49
	$2^3A''$	9.45	3.40	1.40	0.57	0.10	−0.01	0.59	0.12	0.01	−225.622 24
Benzene	SS 1^1A_g	9.30	3.30	1.34	0.51	0.07	−0.02	0.53	0.09	−0.01	−231.850 53
	1^1E_{2g}	9.46	3.34	1.36	0.53	0.09	−0.01	0.55	0.11	0.00	−231.542 70
	1^1B_{2u}	9.41	3.34	1.36	0.52	0.09	−0.01	0.54	0.11	0.00	−231.659 42
	1^1B_{1u}	9.71	3.45	1.40	0.54	0.09	−0.01	0.56	0.11	0.00	−231.628 00
	1^1E_{1u}	9.93	3.60	1.51	0.44	−0.02	−0.15	0.46	0.00	−0.13	−231.605 28
	1^3E_{2g}	9.40	3.32	1.34	0.52	0.09	−0.01	0.54	0.11	0.00	−231.571 34
	1^3B_{1u}	9.49	3.37	1.38	0.54	0.10	0.00	0.56	0.12	0.01	−231.672 26
	1^3B_{2u}	9.71	3.45	1.41	0.54	0.09	−0.02	0.56	0.11	0.00	−231.662 76
	1^3E_{1u}	9.34	3.30	1.34	0.52	0.08	−0.02	0.54	0.10	0.00	−231.691 04
Octatetraene	SS 1^1A_g	12.67	4.43	1.79	0.68	0.11	−0.03	0.71	0.13	−0.01	−310.258 87
	SA 1^1A_g	12.72	4.45	1.80	0.70	0.11	−0.02	0.72	0.14	0.00	−310.263 00
	2^1A_g	12.76	4.45	1.80	0.70	0.12	−0.02	0.73	0.14	0.00	−310.089 39
	3^1A_g	12.81	4.48	1.81	0.71	0.12	−0.01	0.73	0.14	0.01	−310.017 62
	4^1A_g	12.78	4.46	1.80	0.71	0.12	−0.02	0.73	0.14	0.00	−309.979 41
	1^1B_u	12.80	4.48	1.81	0.71	0.12	−0.01	0.74	0.15	0.01	−310.045 65
	2^1B_u	13.16	4.64	1.90	0.73	0.12	−0.01	0.76	0.15	0.01	−310.125 12
	3^1B_u	12.88	4.50	1.83	0.71	0.12	−0.01	0.74	0.15	0.01	−309.953 84
	1^3A_g	12.71	4.44	1.79	0.69	0.11	−0.02	0.72	0.14	0.00	−310.122 20
	1^3B_u	12.69	4.43	1.79	0.69	0.11	−0.02	0.72	0.13	0.00	−310.173 84
MAD		10.15	3.62	1.49	0.58	0.09	0.03	0.60	0.11	0.02	···
SD		10.25	3.65	1.50	0.58	0.10	0.04	0.60	0.11	0.04	···

TABLE II. The excitation energies of low-lying excited states of the chosen organic molecules. The NEVPT2, NEVPT2-F12, and DLPNO-NEVPT2-12 results are deviations (in eV) with respect to that of the CBS limit (in eV).

		NEVPT2			NEVPT2-F12			DLPNO-NEVPT2-F12			
Molecule	States	DZ	TZ	QZ	DZ	TZ	QZ	DZ	TZ	QZ	CBS limit
Furan	2^1A_1	0.16	0.04	0.01	0.00	0.00	−0.01	0.00	0.00	−0.01	6.704
	3^1A_1	0.55	0.26	0.14	−0.03	−0.05	−0.06	−0.03	−0.05	−0.06	8.041
	1^1B_2	0.76	0.42	0.26	−0.04	−0.08	−0.14	−0.04	−0.08	−0.14	5.935
	1^3A_1	0.14	0.04	0.02	0.02	0.01	0.01	0.02	0.01	0.01	5.597
	1^3B_2	0.15	0.05	0.02	0.02	0.01	0.00	0.02	0.01	0.00	4.299
Pyrrole	2^1A_1	0.20	0.07	0.03	0.00	0.00	−0.01	0.00	0.00	−0.01	6.506
	3^1A_1	0.57	0.27	0.16	−0.03	−0.05	−0.06	−0.03	−0.04	−0.06	7.891
	1^1B_2	0.65	0.35	0.22	−0.06	−0.09	−0.10	−0.06	−0.09	−0.10	6.386
	1^3A_1	0.17	0.06	0.03	0.02	0.01	0.01	0.02	0.01	0.01	5.619
	1^3B_2	0.15	0.05	0.03	0.01	0.00	0.00	0.01	0.00	0.00	4.702
Imidazole	$2^1A'$	0.24	0.09	0.04	−0.01	−0.01	−0.02	−0.01	−0.01	−0.02	6.745
	$3^1A'$	0.35	0.11	0.04	−0.06	−0.07	−0.07	−0.06	−0.07	−0.07	6.692
	$4^1A'$	0.39	0.15	0.06	−0.08	−0.10	−0.12	−0.08	−0.10	−0.11	8.406
	$1^1A''$	0.28	0.11	0.06	0.04	0.02	0.01	0.05	0.02	0.01	6.776
	$2^1A''$	0.35	0.15	0.08	0.05	0.01	0.00	0.05	0.02	0.01	7.768
	$1^3A'$	0.20	0.08	0.04	0.03	0.02	0.01	0.03	0.02	0.01	4.722
	$2^3A'$	0.26	0.10	0.05	0.04	0.02	0.02	0.04	0.03	0.02	5.797
	$3^3A'$	0.36	0.14	0.07	0.05	0.03	0.02	0.05	0.03	0.02	6.396
	$4^3A'$	0.25	0.10	0.06	0.03	0.02	0.01	0.04	0.02	0.02	6.968
	$1^3A''$	0.22	0.08	0.05	0.04	0.02	0.01	0.04	0.02	0.02	6.310
	$2^3A''$	0.26	0.10	0.06	0.04	0.01	0.01	0.04	0.02	0.01	7.378
Benzene	1^1E_{2g}	0.16	0.04	0.02	0.02	0.01	0.01	0.02	0.01	0.01	8.377
	1^1B_{2u}	0.11	0.03	0.02	0.01	0.01	0.01	0.01	0.01	0.01	5.200
	1^1B_{1u}	0.41	0.15	0.06	0.03	0.01	0.01	0.03	0.01	0.01	6.055
	1^1E_{1u}	0.63	0.30	0.17	−0.07	−0.10	−0.13	−0.07	−0.09	−0.13	6.674
	1^3E_{2g}	0.10	0.02	0.01	0.01	0.01	0.01	0.01	0.01	0.01	7.597
	1^3B_{1u}	0.19	0.07	0.04	0.03	0.02	0.02	0.03	0.02	0.02	4.851
	1^3B_{2u}	0.40	0.14	0.07	0.03	0.01	0.01	0.03	0.02	0.01	5.109
	1^3E_{1u}	0.04	0.00	0.00	0.01	0.01	0.01	0.01	0.01	0.01	4.340
Octateraene	2^1A_g	0.04	0.00	0.00	0.01	0.00	0.00	0.01	0.00	0.00	4.724
	3^1A_g	0.10	0.02	0.01	0.01	0.01	0.01	0.01	0.01	0.01	6.677
	4^1A_g	0.07	0.00	0.00	0.01	0.01	0.00	0.01	0.01	0.01	7.717
	1^1B_u	0.14	0.04	0.02	0.03	0.02	0.02	0.03	0.02	0.02	5.802
	2^1B_u	0.49	0.20	0.11	0.05	0.02	0.01	0.05	0.02	0.01	3.640
	3^1B_u	0.21	0.07	0.04	0.03	0.02	0.02	0.03	0.02	0.02	8.301
	1^3A_g	0.04	0.00	0.00	0.01	0.01	0.01	0.01	0.01	0.01	3.719
	1^3B_u	0.03	0.00	0.00	0.01	0.00	0.00	0.01	0.00	0.00	2.314
MAD		0.26	0.11	0.06	0.03	0.02	0.03	0.03	0.02	0.03	···
SD		0.32	0.15	0.08	0.03	0.04	0.05	0.03	0.04	0.04	···

the crossover point of the DLPNO-NEVPT2 algorithm vs the conventional NEVPT2 approach is at about 80 atoms.[49] In canonical NEVPT2-F12, the computational cost is dominated by the two-electron integral construction steps, which, involving CABS basis set, are substantially reduced. Thus, the DLPNO method is able to reduce the computational costs of NEVPT2-F12 more significantly than that of NEVPT2. A similar behavior was reported in the DLPNO-MP2-F12 work as well.[50] In Fig. 5, the time of localization and the $[2]_s$ correction for CASSCF are included, which are not linear scaling processes. However, these steps are much faster than

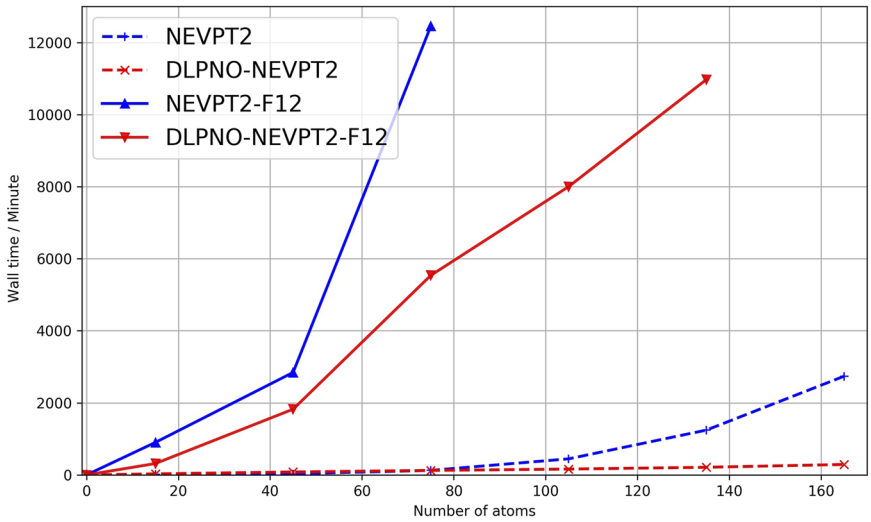

FIG. 5. The wall time of (DLPNO-)NEVPT2 and (DLPNO-)NEVPT2-F12 of $[(C_4SH_3)\text{-}C_nH_{2n}\text{-}(C_4SH_3)]^{2+}$.

the F12 calculations. Thus, the scaling of the DLPNO-NEVPT2-F12 algorithm is 1.38, which is near-linear scaling.

D. Applications

Due to the lack of matching CABS basis sets, currently, all F12 algorithms in ORCA can only deal with molecules composed of atoms of the first three rows. However, most recently, Semidalas and Martin developed the autoCABS method, which is able to generate the CABS basis set for arbitrary orbital basis sets.[79] The accuracy of CABS basis sets generated by autoCABS has been validated using the first- to third-row atoms. The accuracy of autoCABS for transition metals has apparently not yet been tested. Thus, in the present subsection, four truncated cluster models of rhodopsin are computed by DLPNO-NEVPT2-F12. Two 11-cis geometries of retinal chromophores are reported by Park and Shiozaki, which are optimized by CASSCF and extended multi-state (XMS)-CASPT2, respectively.[80] The two models are referred to as CAS-11-cis and PT2-11-cis herein. The third and fourth cluster models are constructed by truncating the structure of 1N3M,[81] which was studied by Rothlisberger *et al.*[82] Only the chromophore and its nearby atoms are included in our cluster models. Two models, consisting of 130 and 180 atoms (dubbed small-11-cis and large-11-cis), are constructed, respectively. The dangling bonds are capped by hydrogen molecules. The resulting chromophore models are optimized by BP86 with the Def2-SVP basis set with a fixed environment. The final geometry is given in the supplementary material. In all calculations of the cluster models, all 12 π-electrons and 12 π-orbitals of the chromophore are included in the active space. The SA-CASSCF(12, 12) over the lowest two singlet states with DZ basis set is used as references in the subsequent DLPNO-NEVPT2-F12 calculations. The 12 CASSCF active MOs and the occupation numbers of small-11-cis are given in the supplementary material, S6.

The absolute energies and the S_1–S_0 gaps of the three models at different levels are given in Table III. The calculations of CAS-11-cis and PT2-11-cis contain 948 basis functions. The energy gaps of the two singlet states predicted by DLPNO-NEVPT2-F12 are 2.22 and 2.45 eV, respectively. The results of PT2-11-cis molecules are consistent with that obtained by XMS-CASPT2. The number of basis functions in the large-11-cis calculations is 3,372, which should be

TABLE III. The energies of the ground states (S_0) and excited states (S_1) of truncated cluster models of rhodopsin computed using DLPNO-NEVPT2 and DLPNO-NEVPT2-12 methods. The total numbers of basis functions are given in parentheses.

	CAS-11-cis (948)		PT2-11-cis (948)		Small-11-cis (2409)		Large-11-cis (3372)	
	S_0 (Hartree)	S_1 (eV)	S_0 (Hartree)	S_1 (eV)	S_0 (Hartree)	S_1 (eV)	S_0 (Hartree)	S_1 (eV)
CASSCF	−868.438 31	3.18	−868.425 89	2.74	−2725.492 23	3.73	−4260.809 91	3.56
DLPNO-NEVPT2	−871.750 01	2.47	−871.753 23	2.24	−2735.358 95	3.56	−4274.906 44	3.36
CASSCF-$[2]_s$	−868.487 99	3.18	−868.475 20	2.74	−2725.638 77	3.74	−4261.019 91	3.52
DLPNO-NEVPT2-F12	−872.430 37	2.45	−872.432 38	2.22	−2737.442 16	3.57	−4277.852 80	3.16
XMS-CASPT2	···	···	−871.108 610	2.34	···	···	···	···

one of the largest MRPT2-F12 calculations ever reported. This calculation is performed on a cluster with one AMD EPYC 7H12 CPU and 1 TB memory. Using 16 processors, the DLPNO-NEVPT2-F12 calculation takes 14.3 days for one root. The main computational effort lies in the calculations of various F12 matrix elements in the S_{iab} subspace, which takes 9.4 days. The energy gaps of the two 1N3M clusters are relatively large, which should be attributed to the structural differences of the retinal. The Schiff base of rhodopsin in the 1N3M model is deprotonated after the constrained optimization. By including more atoms in the active site model, the gap of large-11-cis is about 0.4 eV smaller than that of small-11-cis. Although the absolute energies are improved significantly by the F12 calculations (about 2.94 Hartree), the basis set effect is not pronounced for the excitation energies of the clusters. Nevertheless, these calculations show that the present DLPNO-NEVPT-F12 algorithm can deal with systems of significant size.

IV. CONCLUSION AND OUTLOOK

In the present work, a near linear scaling NEVPT-F12 algorithm, DLPNO-NEVPT2-F12, is developed. The "SparseMap" technique and the idea of DLPNO are used to reduce the computational costs and the storage bottleneck of conventional NEVPT2-F12. The low-lying excited states of a few organic molecules in Thiel's test set are studied using the new method. The DLPNO-NEVPT2-F12 method is able to produce accurate absolute and relative energies as its parent NEVPT2-F12 method. Usually, about 99.9% of NEVPT2-F12 correlation energies can be recovered with much lower computational costs. Provided there is enough memory, our new method should be able to treat systems with about 4,000 basis functions.

There are two major bottlenecks limiting the usage of MRPT2: (a) the high computational cost of canonical correlation methods given the unfavorable scaling with system size and the high computational demands of the necessary integral transformation and (b) the exponential scaling of computational cost for calculations with increasing active space. The first bottleneck has been much alleviated by various local correlation methods, including DLPNO-NEVPT2 and the present method. For the second problem, some of us have found a stable way to extend the calculations to large active spaces with approximate full CI methods.[83–85] Consequently, the DLPNO-NEVPT2 and DLPNO-NEVPT2-F12 algorithms for large systems with large active space references are the logical next steps in this development and will allow accurate NEVPT2 calculations to be performed on large systems. Given the importance of this method, e.g., in molecular magnetism,[86,87] such a development opens fascinating opportunities for computational chemistry.

SUPPLEMENTARY MATERIAL

See the supplementary material for the detailed working equations of DLPNO-NEVPT2-F12 and the basis set convergence trend of benzene.

ACKNOWLEDGMENTS

The authors gratefully acknowledge the financial support by the Max Planck Society and the cluster of excellence (RESOLV, University of Bochum, Grant No. EXC 1069). Y.G. was supported by the Qilu Young Scholar Program from Shandong University and the National Natural Science Foundation of China (Grant No. 22273052). E.F.V. was supported by the U.S. National Science Foundation under Award No. 1931347.

AUTHOR DECLARATIONS

Conflict of Interest

The authors have no conflicts to disclose.

Author Contributions

Yang Guo: Methodology (equal); Software (equal); Validation (equal); Writing – original draft (equal); Writing – review & editing (equal). **Fabijan Pavošević**: Software (equal); Writing – review & editing (equal). **Kantharuban Sivalingam**: Methodology (equal); Writing – original draft (supporting); Writing – review & editing (equal). **Ute Becker**: Software (equal); Writing – review & editing (supporting). **Edward F. Valeev**: Methodology (supporting); Software (supporting); Writing – review & editing (equal). **Frank Neese**: Methodology (equal); Project administration (lead); Software (supporting); Writing – original draft (equal); Writing – review & editing (equal).

DATA AVAILABILITY

The data that support the findings of this study are available within the article and its supplementary material.

REFERENCES

[1] E. R. Davidson and D. Feller, Chem. Rev. **86**, 681 (1986).
[2] T. Helgaker, W. Klopper, H. Koch, and J. Noga, J. Chem. Phys. **106**, 9639 (1997).
[3] K. A. Peterson, D. E. Woon, and T. H. Dunning, Jr., J. Chem. Phys. **100**, 7410 (1994).
[4] A. Halkier, T. Helgaker, P. Jørgensen, W. Klopper, and J. Olsen, Chem. Phys. Lett. **302**, 437 (1999).
[5] W. Kutzelnigg, Theor. Chim. Acta **68**, 445 (1985).
[6] A. Halkier, W. Klopper, T. Helgaker, and P. Jørgensen, J. Chem. Phys. **111**, 4424 (1999).
[7] A. D. Boese, G. Jansen, M. Torheyden, S. Höfener, and W. Klopper, Phys. Chem. Chem. Phys. **13**, 1230 (2011).
[8] W. Klopper, F. R. Manby, S. Ten-No, and E. F. Valeev, Int. Rev. Phys. Chem. **25**, 427 (2006).
[9] W. Klopper and W. Kutzelnigg, Chem. Phys. Lett. **134**, 17 (1987).
[10] W. Kutzelnigg and W. Klopper, J. Chem. Phys. **94**, 1985 (1991).
[11] W. Klopper, R. Röhse, and W. Kutzelnigg, Chem. Phys. Lett. **178**, 455 (1991).
[12] M. Schütz, W. Klopper, H.P. Lüthi and S. Leutwyler, J. Chem. Phys. **103**, 6114 (1995).
[13] W. Klopper and C. C. M. Samson, J. Chem. Phys. **116**, 6397 (2002).
[14] E. F. Valeev, Chem. Phys. Lett. **395**, 190 (2004).
[15] S. Ten-no, Chem. Phys. Lett. **398**, 56 (2004).
[16] D. P. Tew and W. Klopper, J. Chem. Phys. **123**, 074101 (2005).
[17] S. Ten-no, J. Chem. Phys. **121**, 117 (2004).
[18] H.-J. Werner, T. B. Adler, and F. R. Manby, J. Chem. Phys. **126**, 164102 (2007).
[19] H. Fliegl, W. Klopper, and C. Hättig, J. Chem. Phys. **122**, 084107 (2005).
[20] E. F. Valeev and T. D. Crawford, J. Chem. Phys. **128**, 244113 (2008).
[21] H.-J. Werner, G. Knizia, and F. R. Manby, Mol. Phys. **109**, 407 (2011).
[22] D. G. Liakos, R. Izsák, E. F. Valeev, and F. Neese, Mol. Phys. **111**, 2653 (2013).
[23] W. Győrffy, G. Knizia, and H.-J. Werner, J. Chem. Phys. **147**, 214101 (2017).
[24] W. Győrffy and H.-J. Werner, J. Chem. Phys. **148**, 114104 (2018).
[25] R. J. Gdanitz, Chem. Phys. Lett. **210**, 253 (1993).

[26] R. J. Gdanitz, Chem. Phys. Lett. **283**, 253 (1998).

[27] S. Ten-no, Chem. Phys. Lett. **447**, 175 (2007).

[28] R. Haunschild, S. Mao, D. Mukherjee, and W. Klopper, Chem. Phys. Lett. **531**, 247 (2012).

[29] S. Kedžuch, O. Demel, J. Pittner, S. Ten-no, and J. Noga, Chem. Phys. Lett. **511**, 418 (2011).

[30] O. Demel, S. Kedžuch, M. Švaňa, S. Ten-no, J. Pittner, and J. Noga, Phys. Chem. Chem. Phys. **14**, 4753 (2012).

[31] T. Yanai and T. Shiozaki, J. Chem. Phys. **136**, 084107 (2012).

[32] W. Liu, M. Hanauer, and A. Köhn, Chem. Phys. Lett. **565**, 122 (2013).

[33] T. Shiozaki and H.-J. Werner, J. Chem. Phys. **133**, 141103 (2010).

[34] T. Shiozaki, G. Knizia, and H.-J. Werner, J. Chem. Phys. **134**, 034113 (2011).

[35] M. Torheyden and E. F. Valeev, J. Chem. Phys. **131**, 171103 (2009).

[36] L. Kong and E. F. Valeev, J. Chem. Phys. **135**, 214105 (2011).

[37] Y. Guo, K. Sivalingam, E. F. Valeev, and F. Neese, J. Chem. Phys. **147**, 064110 (2017).

[38] H.-J. Werner and F. R. Manby, J. Chem. Phys. **124**, 054114 (2006).

[39] T. B. Adler, H.-J. Werner, and F. R. Manby, J. Chem. Phys. **130**, 054106 (2009).

[40] T. B. Adler and H.-J. Werner, J. Chem. Phys. **130**, 241101 (2009).

[41] T. B. Adler and H.-J. Werner, J. Chem. Phys. **135**, 144117 (2011).

[42] R. Ahlrichs, H. Lischka, V. Staemmler, and W. Kutzelnigg, J. Chem. Phys. **62**, 1225 (1975).

[43] F. Neese, F. Wennmohs, and A. Hansen, J. Chem. Phys. **130**, 114108 (2009).

[44] A. Hansen, D. G. Liakos, and F. Neese, J. Chem. Phys. **135**, 214102 (2011).

[45] C. Riplinger and F. Neese, J. Chem. Phys. **138**, 034106 (2013).

[46] C. Riplinger, B. Sandhoefer, A. Hansen, and F. Neese, J. Chem. Phys. **139**, 134101 (2013).

[47] P. Pinski, C. Riplinger, E. F. Valeev, and F. Neese, J. Chem. Phys. **143**, 034108 (2015).

[48] C. Riplinger, P. Pinski, U. Becker, E. F. Valeev, and F. Neese, J. Chem. Phys. **144**, 024109 (2016).

[49] Y. Guo, K. Sivalingam, E. F. Valeev, and F. Neese, J. Chem. Phys. **144**, 094111 (2016).

[50] F. Pavošević, P. Pinski, C. Riplinger, F. Neese, and E. F. Valeev, J. Chem. Phys. **144**, 144109 (2016).

[51] J. Brabec, J. Lang, M. Saitow, J. Pittner, F. Neese, and O. Demel, J. Chem. Theory Comput. **14**, 1370 (2018).

[52] O. Demel, J. Pittner, and F. Neese, J. Chem. Theory Comput. **11**, 3104 (2015).

[53] F. Menezes, D. Kats, and H.-J. Werner, J. Chem. Phys. **145**, 124115 (2016).

[54] H.-J. Werner, G. Knizia, C. Krause, M. Schwilk, and M. Dornbach, J. Chem. Theory Comput. **11**, 484 (2015).

[55] Q. Ma and H.-J. Werner, J. Chem. Theory Comput. **17**, 902 (2021).

[56] G. Schmitz and C. Hättig, J. Chem. Theory Comput. **13**, 2623 (2017).

[57] C. Krause and H.-J. Werner, Phys. Chem. Chem. Phys. **14**, 7591 (2012).

[58] F. Pavošević, F. Neese, and E. F. Valeev, J. Chem. Phys. **141**, 054106 (2014).

[59] D. P. Tew, B. Helmich, and C. Hättig, J. Chem. Phys. **135**, 074107 (2011).

[60] Q. Ma and H.-J. Werner, J. Chem. Theory Comput. **11**, 5291 (2015).

[61] Q. Ma, M. Schwilk, C. Köppl, and H.-J. Werner, J. Chem. Theory Comput. **13**, 4871 (2017).

[62] F. Pavošević, C. Peng, P. Pinski, C. Riplinger, F. Neese, and E. F. Valeev, J. Chem. Phys. **146**, 174108 (2017).

[63] M. Saitow, U. Becker, C. Riplinger, E. F. Valeev, and F. Neese, J. Chem. Phys. **146**, 164105 (2017).

[64] Y. Guo, C. Riplinger, U. Becker, D. G. Liakos, Y. Minenkov, L. Cavallo, and F. Neese, J. Chem. Phys. **148**, 011101 (2018).

[65] Y. Guo, C. Riplinger, D. G. Liakos, U. Becker, M. Saitow, and F. Neese, J. Chem. Phys. **152**, 024116 (2020).

[66] C. Angeli, R. Cimiraglia, and J.-P. Malrieu, Chem. Phys. Lett. **350**, 297 (2001).

[67] K. G. Dyall, J. Chem. Phys. **102**, 4909 (1995).

[68] C. Angeli, R. Cimiraglia, S. Evangelisti, T. Leininger, and J.-P. Malrieu, J. Chem. Phys. **114**, 10252 (2001).

[69] C. Angeli, R. Cimiraglia, and J.-P. Malrieu, J. Chem. Phys. **117**, 9138 (2002).

[70] F. Neese, Wiley Interdiscip. Rev.: Comput. Mol. Sci. **12**, e1606 (2022).

[71] F. Neese, F. Wennmohs, U. Becker, and C. Riplinger, J. Chem. Phys. **152**, 224108 (2020).

[72] K. A. Peterson, T. B. Adler, and H.-J. Werner, J. Chem. Phys. **128**, 084102 (2008).

[73] K. E. Yousaf and K. A. Peterson, J. Chem. Phys. **129**, 184108 (2008).

[74] L. Kong and E. F. Valeev, J. Chem. Phys. **133**, 174126 (2010).

[75] M. Schreiber, M. R. Silva-Junior, S. P. A. Sauer, and W. Thiel, J. Chem. Phys. **128**, 134110 (2008).

[76] Y. Song, Y. Guo, Y. Lei, N. Zhang, and W. Liu, Top. Curr. Chem. **379**, 43 (2021).

[77] F. N. N. Pansini, A. C. Neto, and A. J. C. Varandas, Theor. Chem. Acc. **135**, 261 (2016).

[78] E. F. Valeev, W. D. Allen, R. Hernandez, C. D. Sherrill, and H. F. Schaefer III, J. Chem. Phys. **118**, 8594 (2003).

[79] E. Semidalas and J. M. L. Martin, J. Comput. Chem. **43**, 1690 (2022).

[80] J. W. Park and T. Shiozaki, Mol. Phys. **116**, 2583 (2018).

[81] Y. Liang, D. Fotiadis, S. Filipek, D. A. Saperstein, K. Palczewski, and A. Engel, J. Biol. Chem. **278**, 21655 (2003).

[82] O. Valsson, P. Campomanes, I. Tavernelli, U. Rothlisberger, and C. Filippi, J. Chem. Theory Comput. **9**, 2441 (2013).

[83] Y. Guo, K. Sivalingam, and F. Neese, J. Chem. Phys. **154**, 214111 (2021).

[84] Y. Guo, K. Sivalingam, C. Kollmar, and F. Neese, J. Chem. Phys. **154**, 214113 (2021).

[85] C. Kollmar, K. Sivalingam, Y. Guo, and F. Neese, J. Chem. Phys. **155**, 234104 (2021).

[86] M. Atanasov, D. Aravena, E. Suturina, E. Bill, D. Maganas, and F. Neese, Coord. Chem. Rev. **289–290**, 177 (2015).

[87] M. Atanasov, N. Spiller, and F. Neese, Phys. Chem. Chem. Phys. **24**, 20760 (2022).